

# A COMPOSITIONAL MODEL TO ASSESS EXPRESSION CHANGES FROM SINGLE-CELL RNA-SEQ DATA

XIUYU MA, KEEGAN KORTHAUER, CHRISTINA KENDZIORSKI, AND MICHAEL A. NEWTON

## 1. INTRODUCTION

The ability to measure genome-wide gene expression at single-cell resolution has accelerated the pace of biological discovery[1]. Overcoming data analysis challenges caused by the scale and unique variation properties of single-cell data will surely fuel further advances in immunology[2], developmental biology[3], cancer[4], and other areas. Computational tools and statistical methodologies created for data of lower-resolution (e.g., bulk RNA-seq) or lower dimension (e.g., flow cytometry) guide our response to the data science demands of new measurement platforms, but they are not adequate for efficient knowledge discovery in this rapidly advancing domain[5].

An important feature of single-cell studies that could be leveraged better statistically is the fact that cells populate distinct, identifiable subtypes determined by lineage history, epigenetic state, the activity of various transcriptional programs, or other distinguishing factors. Lots of efforts have been made to clustering cells into different cell subtypes, SC3[6], CIDR[7] and ZIFA[8]. We hypothesize that such subtype information may be usefully injected into various inference procedures in order to improve their operating characteristics.

Assessing the magnitude and statistical significance of changes in gene expression associated with different cellular conditions has been a central statistical problem in genomics for which new tools specific to the single-cell RNAseq data structure have been deployed: MAST[9], DESEQ2[10], SCDD[11], etc. These tools respond to scRNAseq characteristics, such as high prevalence of zero counts and gene-level multimodality, but none takes explicit advantage of cellular subtype information. We present a simple procedure and supporting theoretical analyses for this purpose. A notable technical innovation is a new prior distribution over pairs of multinomial probability vectors that conveys both marginal Dirichlet conjugacy as well as dependence induced through sharp equalities on aggregated subtype probabilities, which turns out to be key in formulating the posterior probability of changes in expression distributions between conditions.

---

DEPARTMENT OF BIOSTATISTICS AND MEDICAL INFORMATICS, UW MADISON,  
TECHNICAL REPORT TR\*\*\*-V1, FEBRUARY \*\*, 2019.

Using the proposed compositional model, subtypes inferred from whole genome data improve the analysis of gene-level expression. We utilize the mixture of subtypes to characterize transcripts profile and identify differential distributed genes across conditions in an scRNA-seq experiment. Simulation study suggests that the method provides improved power and precision for identifying differentially distributed genes. Performance on empirical data has been investigated through ten previously published experimental data from conquer[12]. We also obtained asymptotic properties of posterior inference.

The proposed scDDboost methodology extends scDD[11], which similarly treats expression data within a condition as a statistical mixture. The extension provided by the present work is to recognize that this mixture is a mixture over cell subtypes. Thus genome-wide data provide information on mixing proportions, thereby providing useful structural information into each gene-level calculation. A software implementation of the proposed methodology is available in the R package SCDDBOOST, at <http://github.com/wiscstatman/scDDboost/>

## 2. MODELING

**2.1. Data structure, sampling model, and parameters.** In modeling scRNASeq data, we imagine that each cell  $c$  falls into one of  $K > 1$  classes, which we think of as subtypes or subpopulations of cells. For notation,  $z_c = k$  means that cell  $c$  happens to be of subtype  $k$ , with the vector  $z = (z_c)$  recording the states of all sampled cells. Knowledge of this class structure prior to measurement is not required, as it will be inferred as necessary from available genomic data. We expect that cells arise from multiple experimental conditions, such as by treatment-control status or some other factors measured at the cell level, but we present our development for the special case of two conditions. Notationally,  $y = (y_c)$  records the experimental condition, say  $y_c = 1$  or  $y_c = 2$  initially: extensions to multiple conditions are discussed in section 6. Let's say condition  $j$  measures  $n_j = \sum_c 1[y_c = j]$  cells, and in total we have  $n = n_1 + n_2$  cells in the analysis. Further let

$$(1) \quad t_k^j = t_k^j(y, c) = \sum_c 1[y_c = j, z_c = k]$$

denote the number of cells of subtype  $k$  in condition  $j$ ; we infer something about these counts using genome-wide data. As for molecular data, the normalized expression of gene  $g$  in cell  $c$ , say  $X_{g,c}$ , is one entry in a typically large GENES by CELLS data matrix  $X$ . Thus, the data structure entails an expression matrix  $X$ , a treatment label vector  $y$ , and a vector  $z$  of latent subtype labels.

We treat subtype counts in the two conditions,  $t^1 = (t_1^1, t_2^1, \dots, t_K^1)$  and  $t^2 = (t_1^2, t_2^2, \dots, t_K^2)$ , as independent multinomial vectors, reflecting the elementary experimental design. Explicitly,

$$(2) \quad t^1|y \sim \text{Multinomial}_K(n_1, \phi) \quad \text{and} \quad t^2|y \sim \text{Multinomial}_K(n_2, \psi)$$

for probability vectors  $\phi = (\phi_1, \phi_2, \dots, \phi_K)$  and  $\psi = (\psi_1, \psi_2, \dots, \psi_K)$  that characterize the populations of cells from which the  $n$  observed cells are sampled. This follows from the more basic sampling model:  $P(z_c = k|y_c = 1) = \phi_k$  and  $P(z_c = k|y_c = 2) = \psi_k$ .

Our working hypothesis, referred to as the *compositional model*, is that any differences in the distribution of expression  $X_{g,c}$  between  $y_c = 1$  and  $y_c = 2$  (i.e., any condition effects) are attributable to differences between the conditions in the underlying composition of cell types; i.e., owing to  $\phi \neq \psi$ . We reckon that cells of any given subtype  $k$  will present data according to a distribution reflecting technical and biological variation specific to that class of cells, regardless of the condition the cell finds itself in. Some care is needed in this, as an overly broad cell subtype (e.g., *epithelial cells*) could have further subtypes that show differential response to some treatment, for example, and so cellular condition (treatment) would then affect the distribution of expression data within the subtype, which is contrary to our working hypothesis. Were that the case, we could have refined the subtype definition to allow a greater number of population classes  $K$  in order to mitigate the problem of within-subtype heterogeneity. A risk in this approach is that  $K$  could approach  $n$ , as if every cell were its own subtype. We find, however, that data sets often encountered do not display this theoretical phenomenon when considering a broad class of within-subtype expression distributions. We revisit the issue in discussion section, but for now proceed assuming that cellular condition affects the composition of subtypes but not the distribution of expression within a subtype.

Within the compositional model, let  $f_{g,k}$  denote the sampling distribution of expression measurement  $X_{g,c}$  assuming that cell  $c$  is from subtype  $k$ . Then for the two cellular conditions, and at some expression level  $x$ , the marginal distributions over subtypes are finite mixtures:

$$f_g^1(x) = \sum_{k=1}^K \phi_k f_{g,k}(x) \quad \text{and} \quad f_g^2(x) = \sum_{k=1}^K \psi_k f_{g,k}(x).$$

In other words,  $X_{g,c}[y_c = j] \sim f_g^j$  and  $X_{g,c}[z_c = k, y_c = j] \sim f_{g,k}$ .

We say that gene  $g$  is *differentially distributed*, denote  $DD_g$  and indicated  $f_g^1 \neq f_g^2$ , if  $f_g^1(x) \neq f_g^2(x)$  for some  $x$ , and otherwise it is equivalently distributed ( $ED_g$ ). Motivated by findings from bulk RNAseq data analysis, we further set each  $f_{g,k}$  to have a negative-binomial form, say with mean  $\mu_{g,k}$  and shape parameter  $\alpha_g$  ([13];[14];[10]). This choice proves to be effective in our numerical experiments though it is not critical to the modeling formulation. \*\*maybe a sentence citing previous papers that use finite mixtures per gene; our angle is to extend by allowing genome-wide data to inform mixing proportions\*\*

We seek a useful methodology to prioritize genes for evidence of  $DD_g$ . Interestingly, even if we have evidence for condition effects on the subtype frequencies, it does not follow that a given gene will have  $f_g^1 \neq f_g^2$ ; that depends on whether or not the subtypes show the right pattern of *differential expression* at  $g$ , to use the standard terminology from bulk RNAseq. For example, if two subtypes have different frequencies between the two conditions ( $\phi_1 \neq \psi_1$  and  $\phi_2 \neq \psi_2$ ) but the same aggregate frequency ( $\phi_1 + \phi_2 = \psi_1 + \psi_2$ ), and also if  $\mu_{g,1} = \mu_{g,2}$  then, other things being equal,  $f_g^1 = f_g^2$  even though  $\phi \neq \psi$ . Simply, a gene that does not distinguish two subtypes will also not distinguish the cellular conditions if those subtypes appear in the same aggregate frequency in the two conditions, regardless of changes in

the individual subtype frequencies. (A second, pedagogical example is presented in the Supplementary Material file.) We formalize the idea in order that our methodology has the necessary functionality. To do so, first consider the parameter space  $\Theta = \{\theta = (\phi, \psi, \mu, \sigma)\}$ , where  $\phi = (\phi_1, \phi_2, \dots, \phi_K)$  and  $\psi = (\psi_1, \psi_2, \dots, \psi_K)$  are as before, where  $\mu = \{\mu_{g,k}\}$  holds all the subtype-and-gene-specific expected values, and where  $\sigma = \{\sigma_g\}$  holds all the gene-specific negative-binomial shape parameters. Critical to our construction are special subsets of  $\Theta$  corresponding to partitions of the  $K$  cell subtypes. A single partition, say  $\pi$ , is a set of mutually exclusive and exhaustive blocks,  $b$ , say, each a subset of  $\{1, 2, \dots, K\}$ , and we write  $\pi = \{b\}$ . Of course, the set  $\Pi$  containing all partitions  $\pi$  of  $\{1, 2, \dots, K\}$  has cardinality that grows rapidly with  $K$ . We carry along an example involving  $K = 7$  cell types, and one three-block partition taken from the set of 877 possible partitions of  $\{1, 2, \dots, 7\}$  (Figure 1).



FIGURE 1. Proportions of  $K = 7$  cellular subtypes in different conditions. Aggregated proportions of subtypes 3 and 4, subtypes 2, 5, and 6, and subtypes 1, and 7 remain same across conditions, while individual subtype frequencies change.

For any partition  $\pi = \{b\}$ , consider aggregate subtype frequencies

$$\Phi_b = \sum_{k \in b} \phi_k \quad \text{and} \quad \Psi_b = \sum_{k \in b} \psi_k,$$

and extend the notation, allowing vectors  $\Phi_\pi = \{\Phi_b : b \in \pi\}$  and similarly for  $\Psi_\pi$ . Recall the partial ordering of partitions based on refinement, and note that as long as  $\pi$  is not the most refined partition (every cell type its own block), then the mapping from  $(\phi, \psi)$  to

$(\Phi_\pi, \Psi_\pi)$  is many-to-one. Further, define sets

$$(3) \quad A_\pi = \{\theta \in \Theta : \Phi_b = \Psi_b \forall b \in \pi\}.$$

and

$$(4) \quad M_{g,\pi} = \{\theta \in \Theta : \mu_{g,k} = \mu_{g,k'} \iff k, k' \in b, b \in \pi\}.$$

Under  $A_\pi$  there are constraints on cell subtype frequencies; under  $M_{g,\pi}$  there is equivalence in the gene-level distribution of expression between certain subtypes. These sets, which are all closed, convex subsets of  $\Theta$ , are precisely the structures needed to address differential distribution  $DD_g$  (and its complement, equivalent distribution,  $ED_g$ ) at a given gene  $g$ , since:

**Theorem 1.** *Let  $C_{g,\pi} = A_\pi \cap M_{g,\pi}$ . For distinct partitions  $\pi_1, \pi_2$ ,  $C_{g,\pi_1} \cap C_{g,\pi_2} = \emptyset$ . Further, at any gene  $g$ , equivalent distribution is*

$$ED_g = \bigcup_{\pi \in \Pi} C_{g,\pi}.$$

With additional probability structure on the parameter space, we immediately obtain from Theorem 1 a formula for local false discovery rates:

$$(5) \quad 1 - P(DD_g|X, y) = P(ED_g|X, y) = \sum_{\pi \in \Pi} P(A_\pi \cap M_{g,\pi}|X, y).$$

*\*\*maybe a sentence and citations about lfdr\*\** The partition representation guides construction of a prior distribution (Section 3.1) and an empirical Bayesian method (Section 2.3) for scoring differential distribution. Setting the stage, Figure 2 shows the dependency structure of the proposed compositional model and the partition-reliant prior specification.

Key to computing the gene-specific local false discovery rate  $P(ED_g|X, y)$  is evaluating probabilities  $P(A_\pi \cap M_{g,\pi}|X, y)$  for any subtype partition  $\pi$  and gene  $g$ . The dependence structure (Figure 2) implies a useful reduction of this quantity, at least conditionally upon subtype labels  $z = (z_c)$ .

**Theorem 2.**  $P(A_\pi \cap M_{g,\pi}|X, y, z) = P(A_\pi|y, z) P(M_{g,\pi}|X, z).$

In what follows, we develop the modeling and computational elements necessary to efficiently evaluate inference summaries (5) taking advantage of Theorems 1 and 2. Roughly, the methodological idea is that subtype labels  $z$  have relatively low uncertainty, and may be estimated from genome-wide clustering of cells in the absence of condition information  $y$ . The modest bit of uncertainty in  $z$  we handle through a computationally efficient randomized clustering scheme. Theorem 2 indicates that our computational task then separates into two parts given  $z$ . On one hand, cell subtype frequencies combine with condition labels to give  $P(A_\pi|y, z)$ . Then gene-level data locally drive the posterior probabilities  $P(M_{g,\pi}|X, z)$  that measure differential expression between subtypes. Essentially, the model provides a specific form of information sharing between genes that leverages the



FIGURE 2. Directed acyclic graph structure of compositional model and partition-reliant prior. The plate on the right side indicates i.i.d. copies over cells  $c$ , conditionally on mixing proportions and mixing components. Observed data are indicated in rectangles/squares, and unobserved variables are in circles/ovals.

compositional structure of single-cell data in order to sharpen our assessments of between-condition expression changes.

**2.2. Method structure and clustering.** We leverage the extensive research on how to cluster cells into subtypes using scRNA-seq data (e.g., SC3[6], CIDR[7], and ZIFA[8]). We propose clustering on the full set of profiles in a way that is blind to the condition label vector  $y$ , in order to have as many cells as possible to inform the subtype structure. We investigated several clustering schemes in numerical experiments and allow flexibility in this choice within the SCDDBOOST software. Associating clusters with subtype labels  $\hat{z}_c$  estimates the actual subtypes  $z_c$ , and prepares us to use Theorems 1 and 2 in order to compute separate posterior probabilities  $P(A_\pi|y, \hat{z})$  and  $P(M_{g,\pi}|X, \hat{z})$  that are necessary for scoring differential distribution. The first probability concerns patterns of cell counts over subtypes in the two conditions, and has a convenient closed form within the *double Dirichlet* model introduced in Section 3.1. The second probability concerns patterns of changes in expected expression levels among subtypes, and this is also conveniently computed for negative-binomial counts using EBSEQ [13]. For completeness we review in Appendix A the empirical Bayes model underlying EBSEQ. Algorithm 1 summarizes how these elements combine to get the posterior probability of differential distribution per gene, conditional on an estimate of the subtype labels.

**Algorithm 1** SCDDBOOST-CORE**Input:**GENES by CELLS expression data matrix  $X = (X_{g,c})$ cell condition labels  $y = (y_c)$ cell subtype labels (estimated)  $\hat{z} = (\hat{z}_c)$ **Output:** posterior probabilities of differential distribution from estimated subtypes

- 1: **procedure** SCDDBOOST-CORE( $X, y, \hat{z}$ )
- 2: number of cell subtypes  $K = \text{length}(\text{unique}(\hat{z}))$
- 3: subtype differential expression:  $\forall g, \pi$  compute  $P(M_{g,\pi}|X, \hat{z})$  using EBSeq[13]
- 4: cell frequency changes:  $\forall \pi$  compute  $P(A_\pi|y, \hat{z})$  using Double Dirichlet model
- 5: posterior probability:  $\forall g, P(\text{ED}_g|X, y, \hat{z}) \leftarrow \sum_{\pi} P(M_{g,\pi}|X, \hat{z}) P(A_\pi|y, \hat{z})$
- 6: **return**  $\forall g, P(\text{DD}_g|X, y, \hat{z}) = 1 - P(\text{ED}_g|X, y, \hat{z})$

We invoke  $K$ -medoids ([15]) as the default clustering method in SCDDBOOST, and customize the cell-cell distance by integrating two measures. The first assembles gene-level information by cluster-based-similarity partitioning ([16]). Separately at each gene, modal clustering ([17] and Appendix B) partitions the cells, and then we define dissimilarity between cells as the proportion of genes at which the cells are assigned to different clusters. A second measure defines dissimilarity by one minus the Pearson correlation between cells, which is computationally inexpensive, less sensitive to outliers than Euclidean distance, and effective at detecting cellular clusters in scRNA-seq([18]). We combine the two measures by a weighted average, with  $w_C = \frac{\sigma_C}{\sigma_C + \sigma_P}$  and  $w_P = 1 - w_C$ . where  $w_C, \sigma_C, w_P, \sigma_P$  are the weights and standard deviations of cluster based distance and Pearson correlation distance accordingly. The resulting distance matrix is  $D = (d_{i,j})$ .

Any clustering method entails classification errors, and so  $\hat{z}_c \neq z_c$  for some cells. To mitigate the effects of this uncertainty, SCDDBOOST averages output probabilities from SCDDBOOST-CORE over randomized clusterings  $\hat{z}^*$ . These are not uniformly random, but rather are generated by applying  $K$ -medoids to a randomized distance matrix  $D^* = (d_{i,j} \times w_{i,j})$ , where  $w_{i,j}$  are unit mean, non-negative weights  $w_{i,j} = 1/(e_i + e_j)$ , and where  $(e_i)$  are independent and identically Gamma( $\hat{a}, \hat{b}$ ) distributed deviates for hyper-parameters  $(\hat{a}, \hat{b})$  derived from  $D$ . We argue (Appendix C) that the distribution of clusterings induced by this simple scheme approximates a Bayesian posterior analysis. Pseudo-code for the resulting SCDDBOOST is in Algorithm (2).

Computations become more intensive the larger is the number  $K$  of cell subtypes. We observe that gene-specific posterior probabilities of differential distribution stabilize when  $K$  is sufficiently large, and we use changes in these profiles to set  $K$ .

In simulations, we observed that averaged adjusted Rand index as well as Rand index of mode of partitions based on randomized distance matrices is higher (better estimation) than that of partition based on original distance matrix (Supplementary Material, \*\*?\*?).  
*MAN to XM: please clarify*

**Algorithm 2** SCDDBOOST

---

**Input:**GENES by CELLS expression data matrix  $X = (X_{g,c})$ cell condition labels  $y = (y_c)$ number of cell subtypes  $K$ number of randomized clusterings  $n_r$ **Output:** posterior probabilities of differential distribution**procedure** SCDDBOOST( $X, y, K, n_r$ )

- 2: distance matrix:  $D = \text{dist}(X) \leftarrow$  pairwise distances between cells (columns of  $X$ )
  - hyper-parameters  $(\hat{a}, \hat{b}) \leftarrow \text{hyper}(D)$
  - 4: **repeat**
  - Gamma noise vector:  $e$ , with components  $\sim \text{Gamma}(\hat{a}, \hat{b})$
  - 6: randomized distance matrix:  $D^* \leftarrow D / (e\mathbf{1}^T + \mathbf{1}e^T)$
  - $\hat{z}^* \leftarrow K\text{-medoids}(D^*)$
  - 8:  $P^* \leftarrow \text{SCDDBOOST-CORE}(X, y, \hat{z}^*)$
  - until**  $n_r$  randomized distance matrices
  - 10: **return**  $\forall \text{genes } g, P(\text{DD}_g | X, y) = \frac{1}{n_r} \sum_{D^*} P_g^*$
- 

**2.3. Double Dirichlet model.** Here we describe the partition-reliant prior  $p(\phi, \psi)$  indicated in Figure 2 and an explicit formula for  $P(A_\pi | y, z)$ . The prior is conjugate to multinomial sampling while also enabling downstream gene-specific inferences about differential distribution. For our purposes, partition-reliance means a spike-slab structure that mixes over partitions  $\pi$  determining patterns of equality of accumulated probabilities through (3):

$$(6) \quad p(\phi, \psi) = \sum_{\pi \in \Pi} \omega_\pi p_\pi(\phi, \psi).$$

Each mixture component  $p_\pi(\phi, \psi)$  has support  $A_\pi$ ; the mixing proportions  $\omega_\pi$  are any non-negative constants summing to one. In numerical experiments we have taken  $\omega_\pi \propto 1$ . *\*\*MAN to XM: what values do we use for alphas and betas?\**To specify component  $p_\pi$ , introduce scalars  $\alpha_k > 0$  for each subtype  $k$ , and  $\beta_b > 0$  for any possible block  $b$ . Extending notation, let  $\alpha_b$  be the vector of  $\alpha_k$  for  $k \in b$ ,  $\beta_\pi$  be the vector of  $\beta_b$  for  $b \in \pi$ ,  $\phi_b$  and  $\psi_b$  be vectors of  $\phi_k$  and  $\psi_k$ , respectively, for  $k \in b$ , and  $\Phi_\pi$  and  $\Psi_\pi$  be the vectors of  $\Phi_b$  and  $\Psi_b$  for  $b \in \pi$ .

Notice that on  $A_\pi$  there is a 1-1 correspondence between pairs  $(\phi, \psi)$  and

$$\left\{ (\tilde{\phi}_b, \tilde{\psi}_b, \Phi_b), \forall b \in \pi \right\},$$

where

$$\tilde{\phi}_b = \frac{\phi_b}{\Phi_b}, \quad \tilde{\psi}_b = \frac{\psi_b}{\Psi_b}, \quad \text{and} \quad \Phi_b = \sum_{k \in b} \phi_k = \sum_{k \in b} \psi_k = \Psi_b.$$



For example,  $\tilde{\phi}_b$  is a vector of conditional probabilities for each subtype given that a cell from the first condition is one of the subtypes in  $b$ . The proposed double-Dirichlet component  $p_\pi$  is determined in this transformed scale by assuming:

$$(7) \quad \Phi_\pi \sim \text{Dirichlet}_{N(\pi)}[\beta_\pi], \text{ and independently, } \tilde{\phi}_b, \tilde{\psi}_b \sim_{\text{i.i.d.}} \text{Dirichlet}_{N(b)}[\alpha_b]$$

where  $N(\pi)$  is the number of blocks in  $\pi$  and  $N(b)$  is the number of subtypes in  $b$ . In other words, on  $p_\pi$ , accumulated probability vectors  $\Phi_\pi$  and  $\Psi_\pi$  are equal between the two source conditions, though the subtype-specific rates  $\phi_k$  and  $\psi_k$  may differ, as would (re-normalized) independent Dirichlet-distributed vectors. (See also Appendix D.) We deduce some properties of the double-Dirichlet model (7), using the Dirichlet-Multinomial conjugacy and the collapsing property ([19]).

**Property 1:** In  $p_\pi(\phi, \psi)$ ,  $\psi$  and  $\phi$  marginally identically distributed as  $\text{Dirichlet}()$ .

**Property 2:** In  $p_\pi(\phi, \psi)$ ,  $\psi$  and  $\phi$  are dependent, unless  $\pi$  is the complete partition in which every cell subtype is its own block.

**Property 3:** The predictive distributions of cell-type counts  $t^1$  and  $t^2$  are all available in closed form.. (1)

Fixing a partition  $\pi$ , let  $t_b^j = \sum_{k \in b} t_k^j$ , for cell conditions  $j = 1, 2$ , record the total numbers of cells accumulated over all types in block  $b \in \pi$ . Following our notation convention,  $t_\pi^j$  is the vector of these counts over  $b \in \pi$ .

Conditional independence of  $t^1$  and  $t^2$  given the block-level totals  $t_\pi^1$  and  $t_\pi^2$  on  $A_\pi$  reflects the possible differential class proportion structure within blocks but between cell conditions. For either cellular group  $j = 1, 2$ , we find, after some simplification, the following Dirichlet-Multinomial masses:

$$(8) \quad p(t^j | t_\pi^j) = \prod_{b \in \pi} \left\{ \left[ \frac{\Gamma(t_b^j + 1)}{\prod_{k \in b} \Gamma(t_k^j + 1)} \right] \left[ \frac{\Gamma(\sum_{k \in b} \alpha_k)}{\prod_{k \in b} \Gamma(\alpha_k)} \right] \left[ \frac{\prod_{k \in b} \Gamma(\alpha_k + t_k^j)}{\Gamma(t_b^j + \sum_{k \in b} \alpha_k)} \right] \right\}$$

and

$$(9) \quad p(t_\pi^1, t_\pi^2 | A_\pi) = \left[ \frac{\Gamma(n_1 + 1) \Gamma(n_2 + 1)}{\prod_{b \in \pi} \Gamma(t_b^1 + 1) \Gamma(t_b^2 + 1)} \right] \left[ \frac{\Gamma(\sum_{b \in \pi} \beta_b)}{\prod_{b \in \pi} \Gamma(\beta_b)} \right] \left[ \frac{\prod_{b \in \pi} \Gamma(\beta_b + t_b^1 + t_b^2)}{\Gamma(n_1 + n_2 + \sum_{b \in \pi} \beta_b)} \right].$$

Let's look at some special cases to dissect this result.

Case 1. If  $\pi$  has a single block equal to the entire set of cell types  $\{1, 2, \dots, K\}$ , then  $t_b^j = n_j$  for both  $j = 1, 2$ , and the second formula reduces, correctly, to  $p(t_\pi^1, t_\pi^2 | A_\pi) = 1$ . Further,

$$p(t^j | t_\pi^j) = \left[ \frac{\Gamma(n_j + 1)}{\Gamma(n_1 + \sum_{k=1}^K \alpha_k)} \right] \left[ \frac{\Gamma(\sum_{k=1}^K \alpha_k)}{\prod_{k=1}^K \Gamma(\alpha_k)} \right] \left[ \prod_{k=1}^K \frac{\Gamma(\alpha_k + t_k^j)}{\Gamma(t_k^j + 1)} \right]$$

which is the well-known Dirichlet-multinomial predictive distribution for counts  $t^j$  [20]. E.g, taking  $\alpha_k = 1$  for all types  $k$  we get the uniform distribution

$$p(t^j|t_\pi^j) = \frac{\Gamma(n_j + 1)\Gamma(K)}{\Gamma(n_j + K)}.$$

Case 2. At the opposite extreme,  $\pi$  has one block  $b$  for each class  $k$ . Then  $t_b^j = z_k^j$ , and  $p(t^j|t_\pi^j) = 1$ , and further, assuming  $\beta_b = \alpha_k$ ,

$$p(t_\pi^1, t_\pi^2|A_\pi) = \left[ \frac{\Gamma(n_1 + 1)\Gamma(n_2 + 1)}{\prod_{k=1}^K \Gamma(t_k^1 + 1)\Gamma(t_k^2 + 1)} \right] \left[ \frac{\Gamma(\sum_{k=1}^K \alpha_k)}{\prod_{k=1}^K \Gamma(\alpha_k)} \right] \left[ \frac{\prod_{k=1}^K \Gamma(\alpha_k + t_k^1 + t_k^2)}{\Gamma(n_1 + n_2 + \alpha_k)} \right].$$

which corresponds to Dirichlet-multinomial predictive distribution for counts  $t^1 + t^2$  since  $t^1$  and  $t^2$  are identical distributed in this case.

\*\*

From (1),  $P(A_\pi|y, z) = P(A_\pi|t^1, t^2)$ .

In order to get the posterior probability  $p(A_\pi|t^1, t^2)$ , we need to calculate

$$\begin{aligned} p(A_\pi|t^1, t^2) &\propto p(A_\pi, t^1, t^2) = \int_{A_\pi} p(t^1, t^2|\phi, \psi)p(\phi, \psi)d\phi d\psi \\ &= \sum_{\pi' \in \Pi} \int_{A_\pi} p(t^1, t^2|\phi, \psi)p_{\pi'}(\phi, \psi)p(A_{\pi'})d\phi d\psi \end{aligned}$$

For simplicity of notation, let  $w(\pi_1, \pi_2) = \int_{A_{\pi_1}} p(t^1, t^2|\phi, \psi)p_{\pi_2}(\phi, \psi)p(A_{\pi_2})d\phi d\psi$ , then  $p(A_\pi|t^1, t^2) \propto \sum_{\pi' \in \Pi} w(\pi, \pi')$ . To calculate component  $w(\pi, \pi')$ , recall refinement and coarseness relationship between partitions, we say a partition  $\tilde{\pi}$  is a refinement of another partition  $\pi$  if  $\forall b \in \pi$  there exists  $s \subset \tilde{\pi}$  such that  $\bigcup_{b' \in s} b' = b$ . We say  $\pi$  is a coarseness of  $\tilde{\pi}$  when  $\tilde{\pi}$  refines  $\pi$ . we have following theorem

**Theorem 3.** *If  $\pi'$  is a refinement of  $\pi$  then  $w(\pi, \pi') = w(\pi', \pi')$  otherwise  $w(\pi, \pi') = 0$*

Consequently, let  $RF(\pi)$  be the collection of finer partition of  $\pi$ , we have the posterior probability:

$$p(A_\pi|t^1, t^2) \propto \sum_{\pi' \in RF(\pi)} w(\pi', \pi')$$

From the prior and model structure

$$w(\pi, \pi) = p(t^1|t_\pi^1)p(t^2|t_\pi^2)p(t_\pi^1, t_\pi^2|A_\pi)p(A_\pi).$$

Regardless of the partition, log scale probabilities are readily evaluated given hyper-parameters  $\{\alpha_k\}$  and  $\{\beta_b\}$  and for cell-type counts  $t^1$  and  $t^2$ .

For asymptotic properties of the posterior probabilities, we demonstrated them in section 6.

### 3. OPERATING CHARACTERISTICS

**3.1. Splatter Simulation.** A simulation study was conducted to assess the performance of scDDboost in identifying DD genes. We simulate data by splatter[21] with approximate 200 cells each condition and 7 subtypes with proportions  $\phi$  and  $\psi$  from Fig 1 satisfying constraints:  $\phi_1 + \phi_2 = \psi_1 + \psi_2$ ,  $\phi_3 + \phi_4 + \phi_5 = \psi_3 + \psi_4 + \psi_5$  and  $\phi_6 + \phi_7 = \psi_6 + \psi_7$ . Each subtype has 10% genes to be differential expressed. We view the differences among subtypes by projecting transcripts profiles of cells into its first two principal components(Fig 2). We observed subtypes are well separated, which is driven by genes with heterogeneous distribution between subtypes.

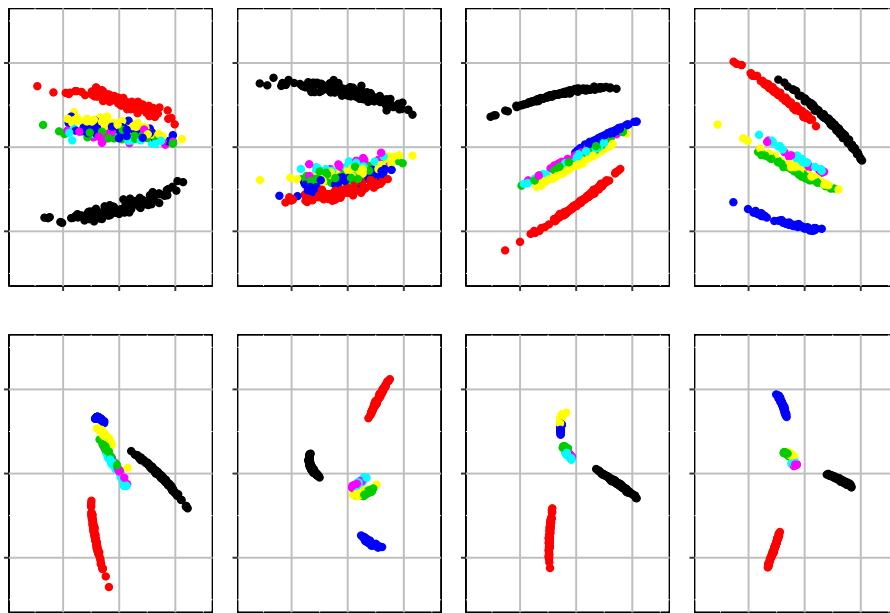


FIGURE 3. first two principal components of transcripts under different parameters for simulated data. Different parameters resulted in different degree of separation of subtypes. We have 4 different settings for hyper-parameters of simulation, each setting has 2 replicates

We determine the number of subtypes by searching a range of candidates(from 1 to 9 based on our empirical experience). Given number of subtypes, we obtain a subtype structure of cells, which will further be fed into computing the posterior probabilities. We visualize the change between posterior probabilities under number of clusters  $i$  and  $i + 1$  ( $i$  from 1 to

8). It typically remains stable when number of cluster is above a number that is smaller than 9 (Fig 3) In the simulated data, the posterior probability become stable when we overestimate the number of subtypes. We found the true number of subtypes is 7 and correctly identify the subtypes of cells.

scDDboost identified most true DD genes, the reason is that mean expression shifts between conditions is not as significant as mean expression shifts between subtypes, which limits the power of MAST and DESeq2. Our approach and scDD considered mixture structure underlying the transcripts but scDD did not use the whole genome information to infer mixture components, which leads to inaccurate clustering at gene level and reduce the power. Under randomized distance, scDDboost gave an accurate estimation of subtypes and thus are more sensitive to the mean expression change among subtypes. We also compare roc curves of scDDboost, scDD, MAST and DESeq2. (Fig 4)

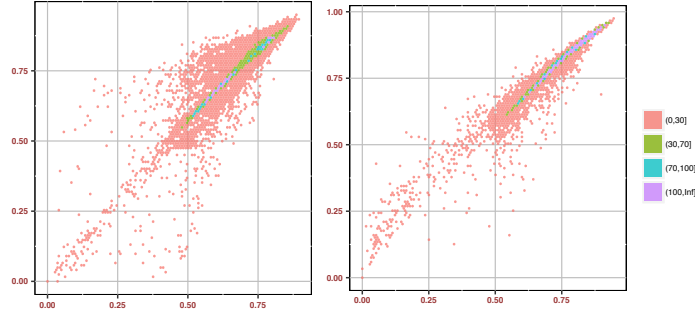


FIGURE 4. comparison of posterior probabilities of being DD among different number of subtypes, when we underestimate the number of subtypes, the difference is huge, see PDD between 6 subtypes and 7 subtypes. There is an approximate horizontal line with massive points at the top of left panel, which indicate that we underestimate lots of DD genes due to underestimate the number of subtypes. While in the case when we overestimate the number of subtypes 7 subtypes vs. 8 subtypes, though inflating PDD but the variation of difference is small, from 6 to 8 subtypes the PDD become more linear related.

Since we are modeling gene transcript within each subtype as negative-binomially distributed and we only test one parameter(mean) change among subtypes. In some scenario, it could be insufficient to model the variability within subtype. Even though there is no mean expression change among subtypes but more subtle distributional change occurred among subtypes changed, EBSeq would fail to detect the discrepancies between subtypes, thus limit power of scDDboost.

### 3.2. Empirical study. \*\*Conquer examples...null and alternative\*\*

We use 13 datasets from conquer[12] to test performance of our method on empirical data. We compare our results with scDD[11], MAST[9] and DESeq2[10], we have also investigated performance of scDDboost under different clustering method, (sc3[6], supplementary) and obtain similar

Data set	Conditions	Number of cells/condition	Organism	Ref
GSE52529	T0 vs T24	96,96	human	[22]
GSE57872	patient1 vs patient2	192,96	human	[23]
GSE48968-GPL13112	BMDC (2h LPS stimulation) vs 6h LPS	96,96	mouse	[24]
GSE60749-GPL13112	serum + LIF vs 2i + LIF	90,94	mouse	[25]
GSE74596	NKT1 vs NTK2	46,68	mouse	[26]
EMTAB2805	G1 vs G2M	96,96	mouse	[27]
GSE71585-GPL13112	Gad2tdTpositive vs Cux2tdTnegative	80,140	mouse	[28]
GSE64016	G1 vs G2	91,76	human	[29]
GSE79102	patient1 vs patient2	51, 89	human	[6]
GSE45719	16-cell stage blastomere vs mid blastocyst cell	50, 60	mouse	[30]
GSE63818	Primordial Germ Cells, developmental stage: 7 week gestation vs Somatic Cells, developmental stage: 7 week gestation	40,26	mouse	[31]
GSE75748	DEC vs EC	64, 64	human	[32]
GSE84465	neoplastic cells vs non-neoplastic cells	546, 664	human	[33]

TABLE 1. datasets used for comparisons of DD analysis under different methods

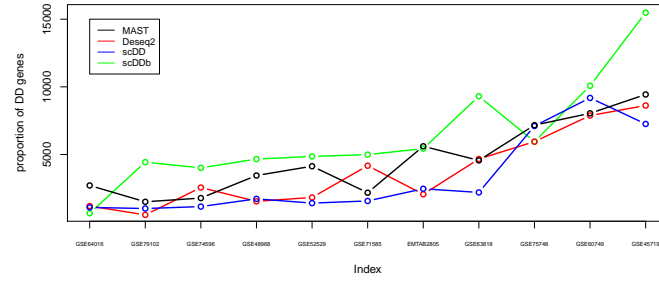


FIGURE 5. number of DD genes with respect to total number of genes identified by each method. Ranked by mean list size

We found that bulk method DESeq2 tends to have the most number of DE genes. But among single cell methods, scDDboost usually identified the most DD genes. Further we observed quite a few genes uniquely identified by scDDboost are likely to have different distribution across conditions. For example, Fig 5, we use violin plot to demonstrate the log expression profiles among DEC and EC.

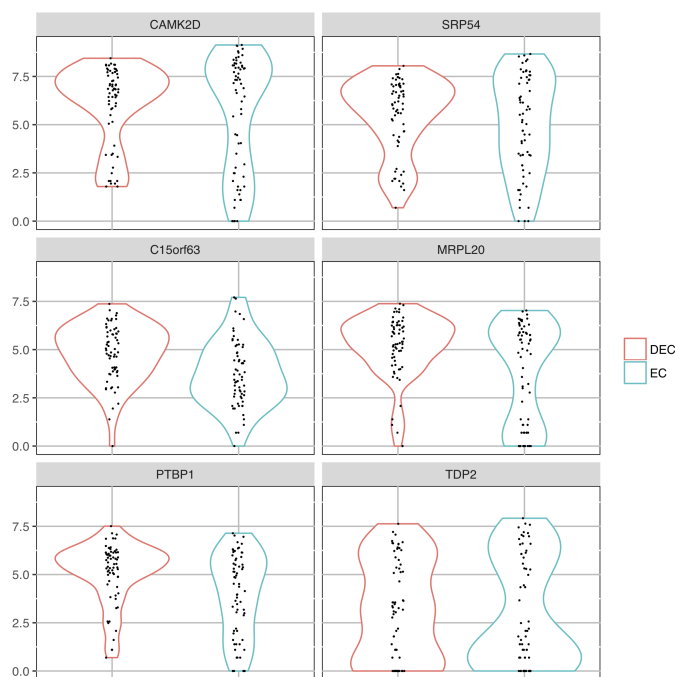


FIGURE 6. Densities of log transformed transcripts, 6 DD genes uniquely identified by scDDboost, for data GSE75748, DEC vs. EC, We observe some of the genes are different distributed across conditions.

**3.3. Empirical study: null cases.** Although bulk methods seems to be the most powerful one, we found it also has a higher false discovery rate comparing to single cell methods. We validate false discovery rate on ten null datasets from table 1. For each null dataset, we randomly split the cells from one condition into two subsets and test difference of gene expression between those subsets. Since the two subsets of cells actually came from same condition, there should not be any differential distributed genes, any positive call would be a false positive. We repeat the random split and testing for five times on each null data set. We evaluate the type I error control for the methods returning nominal p-values, by recording the fraction of genes(with a valid p-value) that are assigned a nominal p-value below 0.05 (Fig 6).

scDDboost could control FDR since we assume cells are sampled from population composed of different subtypes. Cells from one subtype are equal likely to be assigned to either one of the two subsets. Consequently, it is very likely that proportions of subtypes remain unchanged among the two subsets.

Data set	Conditions	Number of cells/condition	Organism
GSE57872null	patient1	96,96	human
GSE52529null	T0	48, 48	human
GSE48968-GPL13112null	BMDC (2h LPS stimulation)	48,48	mouse
GSE60749-GPL13112null	v6.5 mouse embryonic stem cells, culture conditions: 2i+LIF	45,45	mouse
GSE74596null	NKT1	23,23	mouse
EMTAB2805null	G1	48,48	mouse
GSE71585-GPL13112null	Gad2tdTpositive	40,40	mouse
GSE64016null	G1	46,45	human
GSE79102null	patient1	26, 25	human

TABLE 2. datasets used for null cases, as cells are coming from same biological condition, there should not be any differential distributed genes, any positive call is false positive

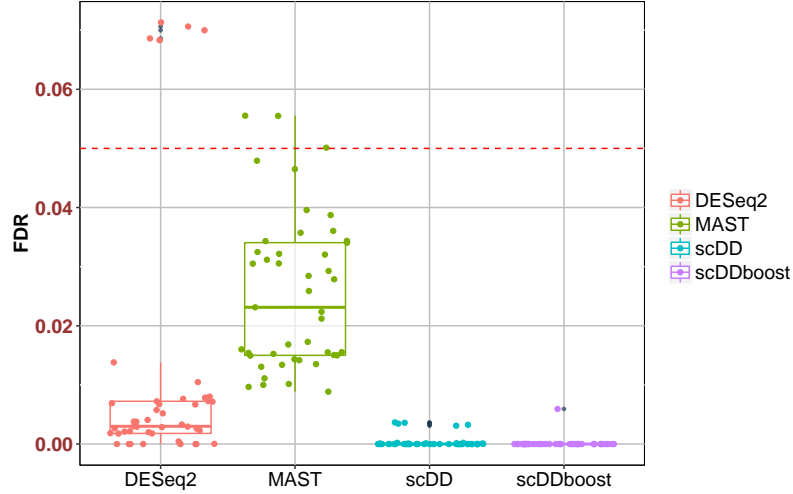


FIGURE 7. FDR of scDDboost, scDD, MAST and DESeq2 on null dataset from table 1, DESeq2 usually identify a lot but may lose the control of type I error. While other single cell methods could control FDR.

**3.4. Number of subtypes.** From our empirical experience, it is typical  $K$  will not be larger than 8. We demonstrate the change of posterior probabilities of differential distribution given different number of subtypes at data GSE75748 and GSE48968. In both cases, if allowing one more subtype would result in a lot increases in posterior probabilities, which



suggests that the number of subtypes is underestimated since we found more distribution differences between conditions given one more mixture component. If posterior inference is stable after increasing the number of subtypes, then we consider previous number of subtypes to be optimal.

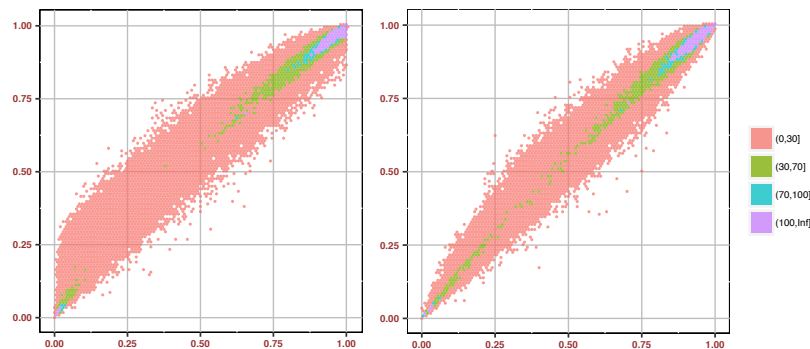


FIGURE 8. selecting number of subtypes for data GSE57872, we observe posterior probabilities become stable at more than 6 subtypes. Since increasing number of subtypes tends to decrease sample size of each subtypes, make complicate constraints for equivalent distribution and inflate estimated PDD. We select number of subtypes to be 7

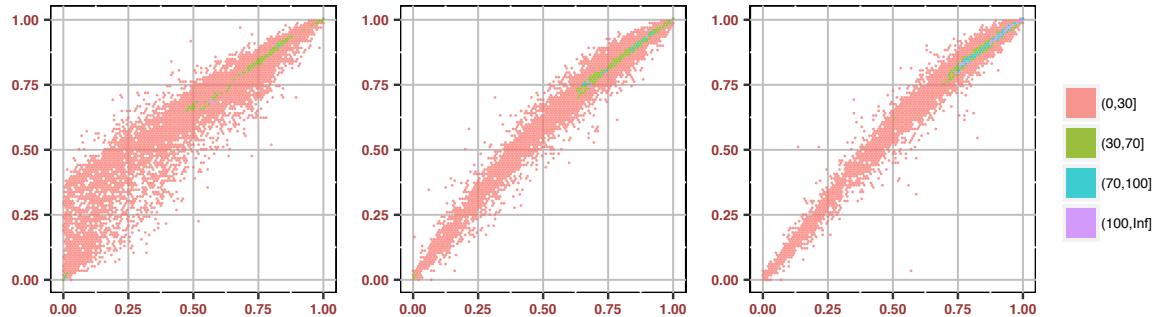


FIGURE 9. selecting number of subtypes for data GSE48968, we observe posterior probabilities become stable at more than 5 subtypes

**3.5. Bursting parameters.** D3E[34] is a distributional method that can identify bursting parameters of transcripts. Rate of promoter activation, rate of promoter inactivation and the rate of transcription when the promoter is in the active state are estimated by D3E. We investigate DD genes identified by scDDboost and their change of those three parameters on dataset EMTAB2805

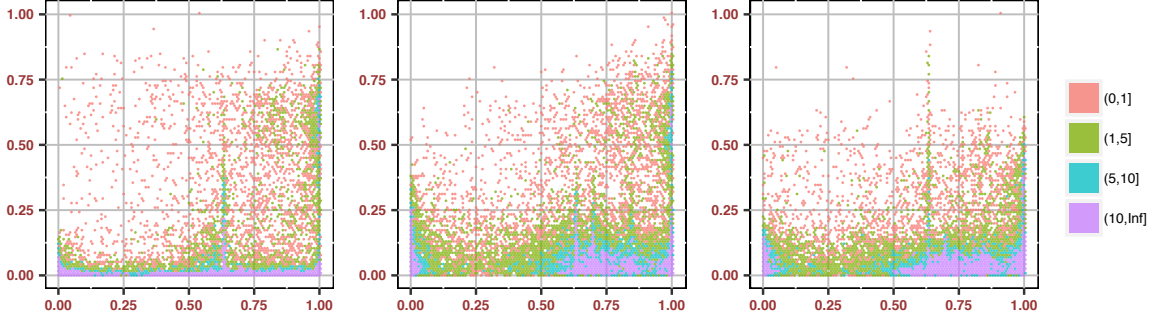


FIGURE 10. D3E method will estimate 3 bursting parameters probability of a gene being on (a) and off (b) and the expression rate when the gene expression is on (c), we plot the hexbin plot of probability of a gene being DD under our method v.s. the absolute value of log fold change of a, b and c across the two conditions accordingly. The log fold change is scaled by dividing the largest log fold change so that ends up in a value between 0 and 1 Here we use the GSE71585 data

We observed that DD genes identified by scDDboost tends to have similar transcription rate when the promoter is active across condition, while there are lots of variabilities in the action and inactivation rate. Estimations from D3E reveals that the major factor to drive DD genes are activation and inactivation rate (proportions of different subtypes), it make sense to consider mixture model like scDDboost.

#### 4. THEORETICAL ISSUES

**4.1. Posterior consistency.** Under some parameters settings, the double dirichlet prior will have limited resolution and lead to inconsistency of posterior probabilities, which we investigate with the following asymptotic analysis.

We first give the expression of posterior probability. Since there is no information favorable of any particular  $A_\pi$ , we select discrete uniform distribution as the prior for it, then the posterior probability is

$$(10) \quad p(A_\pi | t^1, t^2) = c * \sum_{\pi' \text{ refines } \pi} p(t^1 | t_{\pi'}^1) p(t^2 | t_{\pi'}^2) p(t_{\pi'}^1, t_{\pi'}^2 | A_{\pi'})$$

for a normalizing constant  $\frac{1}{c} = \sum_{\pi' \in \Pi} p(t^1 | t_{\pi'}^1) p(t^2 | t_{\pi'}^2) p(t_{\pi'}^1, t_{\pi'}^2 | A_{\pi'})$ .

Let  $\Omega = \{(\phi, \psi) : \sum_{i=1}^K \phi_i = \sum_{i=1}^K \psi_i = 1, \phi_i \geq 0, \psi_i \geq 0, i = 1, \dots, K\}$  be the whole space. There is a subset of  $\Omega$  we lack posterior inference. Let us first see an example:

In Fig 10, there are four subtypes, the rectangle with magenta boundary is a simplex  $A_{\pi_1} = \{(\phi, \psi) : \phi_1 + \phi_2 = \psi_1 + \psi_2\}$ , the rectangle with blue boundary is a simplex  $A_{\pi_2} =$



FIGURE 11. Four subtypes of cells, simplexes of  $(\phi, \psi)$  satisfying different constraints.

$\{(\phi, \psi) : \phi_1 + \phi_3 = \psi_1 + \psi_3\}$ . The green line refers to  $A_{\pi_3} = \{(\phi, \psi) : \phi_1 = \psi_1, \phi_2 = \psi_2\}$ , the yellow line refers to  $A_{\pi_4} = \{(\phi, \psi) : \phi_1 = \psi_1, \phi_3 = \psi_3\}$ , the purple line refers to  $A_{\pi_5} = \{(\phi, \psi) : \phi_1 + \phi_2 = \psi_1 + \psi_2, \phi_1 + \phi_3 = \psi_1 + \psi_3\}$ , which is the intersection of  $A_{\pi_1}$  and  $A_{\pi_2}$ , and finally the black dot which is the intersection of those three lines refers to the simplex with finest partitions,  $\phi_i = \psi_i, \forall i = 1, \dots, 4$ . We lack posterior inference for  $(\phi, \psi)$  along the purple line except the black dot. While on the green line, yellow line and black dot, we have consistent posterior inference (theorem 2). To explain why some space lacking posterior inference and define such space, we define a special subset  $A_\pi^*$  of simplex  $A_\pi$ .  $A_\pi^* = A_\pi \setminus \bigcup_{\tilde{\pi} \text{ is not coarser than } \pi} A_{\tilde{\pi}}$ ,  $A_\pi^*$  is obtained by removing all intersection with other  $A_{\tilde{\pi}}$  (excluding those  $A_{\tilde{\pi}}$  that is superset of  $A_\pi$ ) from  $A_\pi$ . Since we removed those intersection parts. It is intuitive that  $A_\pi^*$  will be disjoint subsets of  $\Omega$ .

**Proposition 1.** *if  $\pi_1 \neq \pi_2$ , then  $A_{\pi_1}^* \cap A_{\pi_2}^* = \emptyset$*

Let  $Q = \Omega \setminus \bigcup_{\pi \in \Pi} A_\pi^*$ , and we have following proposition of the existence of  $Q$ .

**Proposition 2.** *Let  $K$  be number of subtypes. When  $K > 3, Q \neq \emptyset$ , when  $K \leq 3, Q = \emptyset$*

When the number of subtypes is bigger than three, we lack posterior inference on  $Q$ . To

see that we can rewrite  $A_\pi^*$  as  $A_\pi^* = A_\pi \setminus \bigcup_{\tilde{\pi} \text{ is not coarser than } \pi} (A_{\tilde{\pi}} \cap A_\pi)$ ,  $\tilde{\pi}$  is not coarser than  $\pi$ , which is equivalently to say  $\pi$  is not refinement of  $\tilde{\pi}$ . By lemma 1,  $A_{\tilde{\pi}} \cap A_\pi$  is a lower dimensional subset of  $A_\pi$ . So  $A_\pi \setminus A_\pi^*$  is a lower dimensional subset of  $A_\pi$ . For posterior on  $Q$ , it degenerates to integral on a lower dimensional subset of the simplex associating with densities, which will vanish

**Proposition 3.** *When  $K > 3$ ,  $p(Q|z^1, z^2) = 0$*

But for  $(\phi, \psi) \in \Omega \setminus Q$ , we have consistent posterior inference. Assuming  $\alpha_i = 1, \forall i$  in (2) and  $\beta_b = \sum_{i \in b} \alpha_i$  in (3), plug in (4) then we have simplified

$$(11) \quad p(A_\pi | t^1, t^2) = \frac{1}{c'} \sum_{\pi' \in \text{RF}(\pi)} \prod_{b \in \pi'} \frac{\Gamma(\beta_b + t_b^1 + t_b^2)}{\Gamma(\beta_b + t_b^1) \Gamma(\beta_b + t_b^2)}$$

$c' = c / \frac{\Gamma(n+1)\Gamma(n+1)\Gamma(K)}{\Gamma(2n+K)}$  And we have theorem 3.

**Theorem 4.** *Let  $n = \min(n_1, n_2)$  be the smaller number of cells of two conditions and  $n_1 = O(n_2)$ , when parameter  $(\phi, \psi) \in \Omega \setminus Q$  we have*

$$p(A_\pi | t^1, t^2) \xrightarrow[n \rightarrow \infty]{a.s.} \begin{cases} 1 & \text{if } (\phi, \psi) \in A_\pi \\ 0 & \text{otherwise} \end{cases}$$

Things become more complicate when  $(\phi, \psi)$  falling into  $Q$ , we know  $p(Q|t^1, t^2)$  vanishes, but  $p(A_\pi | t^1, t^2)$  may not.

Recall  $N(\pi)$  represents number of blocks  $b$  in  $\pi$ . Let  $S = \{\pi, (\phi, \psi) \in A_\pi\}$ , which is the collection of partitions whose associated simplexes covering  $(\phi, \psi)$ . Let  $N^* = \max_{\pi \in S} N(\pi)$ , which is the max number of blocks of partitions from  $S$ . Let  $S^* = \{\pi, (\phi, \psi) \in A_\pi \text{ and } N(\pi) = N^*\}$ , which is the collection of partitions that covering  $(\phi, \psi)$  with number of blocks equal to the max number  $N^*$ .

For example, when  $K = 7$ , For a  $(\phi, \psi) \in A_{\pi_1} \cap A_{\pi_2} \cap A_{\pi_3}$ ,  $\pi_1 = \{\{1, 2, 3\}, \{4, 5, 6, 7\}\}$ ,  $\pi_2 = \{\{1, 6, 7\}, \{2, 4\}, \{3, 5\}\}$ ,  $\pi_3 = \{\{1, 2, 3, 4, 5, 6\}\}$ , and also  $(\phi, \psi)$  does not belong to any other simplex  $A_\pi$ . Then  $S = \{\pi_1, \pi_2, \pi_3\}$ ,  $N^* = 3$ ,  $S^* = \{\pi_2\}$ .

Denote components from right hand side of (5):  $\frac{1}{c'} \prod_{b \in \pi} \frac{\Gamma(\beta_b + t_b^1 + t_b^2)}{\Gamma(\beta_b + t_b^1) \Gamma(\beta_b + t_b^2)} = J(t^1, t^2, \pi)$ . We have theorem 4.

**Theorem 5.** *Following the setting in theorem 2, when parameter  $(\phi, \psi) \in Q$ , and we have*

$$J(t^1, t^2, \pi) \xrightarrow[n \rightarrow \infty]{a.s.} \begin{cases} m(\pi) & \pi \in S^* \\ 0 & \text{otherwise} \end{cases}$$

$$\text{and } \sum_{\pi \in S^*} m(\pi) = 1, m(\pi) > 0$$

proofs are in the appendix.

Still using above example, in limiting case, we have  $p(A_{\pi_3}|t^1, t^2) = 1$ ,  $p(A_{\pi_2}|t^1, t^2) = 1$  and  $p(A_{\pi_1}|t^1, t^2) = 0$ . When the DE pattern is  $B_{\pi_1}$  for some genes. Since our underestimation of  $p(A_{\pi_1}|z^1, z^2) = 0$ , we will falsely classify those genes as differential distributed.

The asymptotic properties help us gain insight of the performance of our approach, scD-Dboost may work poorly, when  $(\phi, \psi) \in Q$ , we may underestimate the posterior probability of true proportion change pattern, which reduce the posterior probabilities of true negative and enlarge false positive rate.

**4.2. Random weighting.** In this section, we gave an intuitive justification for consistency between bayesian framework clustering analysis and random weighting procedure. A full bayesian analysis for clustering needs to specify the density of data given the partition. Specifically, in single cell analysis we need to know the density of transcripts of genes given the partitions which requires understanding of co-expression and dependence between genes. Instead of trying to untangle the mystery behind the dependence of genes, we consider following approximation

$$P(\text{Partition}|X) \leftarrow P(\text{Partition}|D) \leftarrow P(\Delta|D) \leftarrow D/W$$

where  $D$  is the estimated distance matrix of  $X$ ,  $\Delta$  is the true distance of  $X$  and  $W$  is randomly distributed matrix of weights. We conjecture that the probability of partitions given data can be approximated by switching conditioning on data to conditioning on the estimated distance of data. As distance matrix typically gave the geometrical structure between elements which can be used to infer how likely a partition is. In addition, partition can be obtained by distance based clustering algorithm (K-medoids) on true distance matrix  $\Delta$ . To approximate distribution  $(\Delta|D)$ , we use our random weighting procedure, namely sampling a weighting matrix  $W$  first and then do the component-wisely dividing of original distance matrix  $D$  by  $W$ .

We gave a brief justification for this approximation, suppose units  $i$  and  $j$  are merged into a common cluster if (and only if)  $d_{i,j} < c$ . Then  $P(d_{i,j}^* < c) = P(w_{i,j} > c/d_{i,j})$ ,  $w_{i,j} \sim \text{Gamma}(a, b)$ . From Bayesian perspective, given the true distance  $\Delta_{i,j}$ ,  $d_{i,j}|\Delta_{i,j} \sim \text{Gamma}(a_1, a_1/\Delta_{i,j})$ , so that the sampling mean of  $d_{i,j}$  is  $\Delta_{i,j}$ . Further, for simplicity we ignore any issues about the  $d$ 's or  $\Delta$ 's being true distances. The condition for qualifiable distance matrix is the triangle inequality among the pairwise distances, such condition would not affect our clustering results too much. But, a simple analysis might suppose that a-priori  $1/\Delta_{i,j} \sim \text{Gamma}(a_0, d_0)$ . The scaling is such that  $E(1/\Delta_{i,j}) = a_0 d_0$ . The posterior, by conjugacy, has  $1/\Delta_{i,j}|d_{i,j} \sim \text{Gamma}(a_0 + a_1, d_0 + a_1 d_{i,j})$ . Then the posterior

probability that  $i$  and  $j$  should be clustered is the posterior probability that  $\Delta_{i,j} < c$ , which is  $P(\text{Gamma}(a_0 + a_1, (a_0 + a_1)) > (d_0 + a_1 * d_{i,j}) / (a_0 + a_1) * 1/c)$ , parameters  $(a_0, d_0, a_1)$  are estimated from maximizing the marginal likelihood of  $d_{i,j}$ .

In order to match the posterior probability that elements  $i$  and  $j$  belongs to the same cluster through the simple bayesian analysis to random weighting, which is equivalently to match

$$P(\Delta_{i,j} < c | d_{i,j}) = P(1/\Delta_{i,j} > 1/c | d_{i,j})$$

and

$$P(d_{i,j}/w_{i,j} < c | d_{i,j}) = P(w_{i,j}/d_{i,j} > 1/c | d_{i,j})$$

yielding  $a = a_0 + a_1$  and  $b = a_1$ . Therefore, we gave a way of modeling the distribution of weights such that partition based on random generated distance  $D/W$  would approximate the partition given data based on a full bayesian framework.

## 5. DISCUSSION

We have presented scDDboost, a compositional model for detecting differential distributed genes from scRNA-seq data. To account for the over-dispersion and multi-modality of single-cell data, scDDboost modeled transcripts as mixture distributed. Unlike previous invented methods (e.g. Deseq2, MAST and scDD), which conducts genewise DD test in an isolated manner. scDDboost make whole genome information shared at gene level by further assuming the mixture distribution of transcripts is a mixture over the subtypes of cells. Another advantage of scDDboost is its' flexibility to allow user specified clustering methods of cells, with more and more studies of the scRNA-seq data, there will be more accurate distance matrix between cells, which will yield better estimation of subtypes and inference of DD genes. We combine estimations of changes of subtypes' proportions across conditions and changes of mean expressions across subtypes to infer distributional changes of transcripts. To estimate changes of subtypes' proportions across conditions, we use empirical Bayes and developed a double Dirichlet prior distribution. We invented a random weighting scheme that stabilize our DD inference as well as approximating the results as if we have done a fully bayesian clustering analysis based on Dirichlet prior. We demonstrated that scDDboost outperforms existing approaches in simulation and tends to be more powerful than existing methods on a wide range of public available empirical datasets.

One limitation of scDDboost is that current EBseq inference of the DE patterns is computationally not feasible for big number of subtypes. Given the noise level among the single cell data and especially if we want to identify DD genes among conditions containing thousands of cells, allowing a big number of subtypes would make cells under same subtype more homogeneous and result in a more accurate estimations for the distribution of

transcripts. Further research is needed for acceleration of EBseq, one direction is to reduce the calculation on those patterns that would have small posterior probabilities.

## REFERENCES

- [1] T. Nawy, “Single-cell sequencing,” *Nature Methods*, vol. 11, pp. 18 EP –, 12 2013. [Online]. Available: <http://dx.doi.org/10.1038/nmeth.2771>
- [2] E. Papalexi and R. Satija, “Single-cell rna sequencing to explore immune cell heterogeneity,” *Nature Reviews Immunology*, vol. 18, pp. 35 EP –, 08 2017. [Online]. Available: <http://dx.doi.org/10.1038/nri.2017.76>
- [3] J. C. Marioni and D. Arendt, “How single-cell genomics is changing evolutionary and developmental biology,” *Annual Review of Cell and Developmental Biology*, vol. 33, no. 1, pp. 537–553, Oct 2017, pMID: 28813177. [Online]. Available: <https://doi.org/10.1146/annurev-cellbio-100616-060818>
- [4] N. E. Navin, “The first five years of single-cell cancer genomics and beyond,” *Genome Research*, vol. 25, no. 10, pp. 1499–1507, 10 2015. [Online]. Available: <http://www.ncbi.nlm.nih.gov/pmc/articles/PMC4579335/>
- [5] R. Bacher and C. Kendzierski, “Design and computational analysis of single-cell rna-sequencing experiments,” *Genome Biology*, vol. 17, no. 1, p. 63, 2016. [Online]. Available: <https://doi.org/10.1186/s13059-016-0927-y>
- [6] V. Y. Kiselev, K. Kirschner, M. T. Schaub, T. Andrews, A. Yiu, T. Chandra, K. N. Natarajan, W. Reik, M. Barahona, A. R. Green, and M. Hemberg, “Sc3: consensus clustering of single-cell rna-seq data,” *Nature Methods*, vol. 14, pp. 483 EP –, 03 2017. [Online]. Available: <http://dx.doi.org/10.1038/nmeth.4236>
- [7] P. Lin, M. Troup, and J. W. K. Ho, “Cidr: Ultrafast and accurate clustering through imputation for single-cell rna-seq data,” *Genome Biology*, vol. 18, no. 1, p. 59, 2017. [Online]. Available: <https://doi.org/10.1186/s13059-017-1188-0>
- [8] E. Pierson and C. Yau, “Zifa: Dimensionality reduction for zero-inflated single-cell gene expression analysis,” *Genome Biology*, vol. 16, no. 1, p. 241, 2015. [Online]. Available: <https://doi.org/10.1186/s13059-015-0805-z>
- [9] G. Finak, A. McDavid, M. Yajima, J. Deng, V. Gersuk, A. K. Shalek, C. K. Slichter, H. W. Miller, M. J. McElrath, M. Prlic, P. S. Linsley, and R. Gottardo, “Mast: a flexible statistical framework for assessing transcriptional changes and characterizing heterogeneity in single-cell rna sequencing data,” *Genome Biology*, vol. 16, no. 1, p. 278, 2015. [Online]. Available: <https://doi.org/10.1186/s13059-015-0844-5>
- [10] M. I. Love, W. Huber, and S. Anders, “Moderated estimation of fold change and dispersion for rna-seq data with deseq2,” *Genome Biology*, vol. 15, no. 12, p. 550, 2014. [Online]. Available: <https://doi.org/10.1186/s13059-014-0550-8>
- [11] K. D. Korthauer, L.-F. Chu, M. A. Newton, Y. Li, J. Thomson, R. Stewart, and C. Kendzierski, “A statistical approach for identifying differential distributions in single-cell rna-seq experiments,” *Genome Biology*, vol. 17, no. 1, p. 222, 2016. [Online]. Available: <https://doi.org/10.1186/s13059-016-1077-y>

- [12] C. Soneson and M. D. Robinson, “Bias, robustness and scalability in differential expression analysis of single-cell rna-seq data,” *bioRxiv*, 2017. [Online]. Available: <https://www.biorxiv.org/content/early/2017/05/28/143289>
- [13] N. Leng, J. A. Dawson, J. A. Thomson, V. Ruotti, A. I. Rissman, B. M. G. Smits, J. D. Haag, M. N. Gould, R. M. Stewart, and C. Kendziorski, “Ebseq: an empirical bayes hierarchical model for inference in rna-seq experiments,” *Bioinformatics*, vol. 29, no. 8, pp. 1035–1043, 2013. [Online]. Available: <http://dx.doi.org/10.1093/bioinformatics/btt087>
- [14] S. Anders and W. Huber, “Differential expression analysis for sequence count data,” *Genome Biology*, vol. 11, no. 10, pp. R106–R106, 2010. [Online]. Available: <http://www.ncbi.nlm.nih.gov/pmc/articles/PMC3218662/>
- [15] L. Kaufman and P. Rousseeuw, *Clustering by means of medoids*. North-Holland, 1987.
- [16] A. Strehl and J. Ghosh, “Cluster ensembles — a knowledge reuse framework for combining multiple partitions,” *J. Mach. Learn. Res.*, vol. 3, pp. 583–617, Mar. 2003. [Online]. Available: <https://doi.org/10.1162/153244303321897735>
- [17] D. B. Dahl, “Modal clustering in a class of product partition models,” *Bayesian Anal.*, vol. 4, no. 2, pp. 243–264, 06 2009. [Online]. Available: <https://doi.org/10.1214/09-BA409>
- [18] T. Kim, I. R. Chen, Y. Lin, A. Y.-Y. Wang, J. Y. H. Yang, and P. Yang, “Impact of similarity metrics on single-cell rna-seq data clustering,” *Briefings in Bioinformatics*, p. bby076, 2018. [Online]. Available: <http://dx.doi.org/10.1093/bib/bby076>
- [19] B. Dickey J., Lientz, “The weighted likelihood ratio, sharp hypotheses, and the order of a markov chain.” *Ann. Math. Statist.*, vol. 41, no. 1, p. 214, 1970. [Online]. Available: <https://projecteuclid.org/euclid.aoms/1177697203>
- [20] U. Wagner and A. Taudes, “A multivariate polya model of brand choice and purchase incidence,” *Marketing Science*, vol. 5, no. 3, pp. 219–244, Aug. 1986. [Online]. Available: <http://dx.doi.org/10.1287/mksc.5.3.219>
- [21] L. Zappia, B. Phipson, and A. Oshlack, “Splat: simulation of single-cell rna sequencing data,” *Genome Biology*, vol. 18, no. 1, p. 174, 2017. [Online]. Available: <https://doi.org/10.1186/s13059-017-1305-0>
- [22] C. Trapnell, D. Cacchiarelli, J. Grimsby, P. Pokharel, S. Li, M. Morse, N. J. Lennon, K. J. Livak, T. S. Mikkelsen, and J. L. Rinn, “The dynamics and regulators of cell fate decisions are revealed by pseudotemporal ordering of single cells,” *Nature biotechnology*, vol. 32, no. 4, pp. 381–386, 04 2014. [Online]. Available: <https://www.ncbi.nlm.nih.gov/pubmed/24658644>
- [23] A. P. Patel, I. Tirosh, J. J. Trombetta, A. K. Shalek, S. M. Gillespie, H. Wakimoto, D. P. Cahill, B. V. Nahed, W. T. Curry, R. L. Martuza, D. N. Louis, O. Rozenblatt-Rosen, M. L. Suvà, A. Regev, and B. E. Bernstein, “Single-cell rna-seq highlights intratumoral heterogeneity in primary glioblastoma,” *Science*, vol. 344, no. 6190, pp. 1396–1401, 2014. [Online]. Available: <http://science.sciencemag.org/content/344/6190/1396>



- [24] A. K. Shalek, R. Satija, J. Shuga, J. J. Trombetta, D. Gennert, D. Lu, P. Chen, R. S. Gertner, J. T. Gaubblomme, N. Yosef, S. Schwartz, B. Fowler, S. Weaver, J. Wang, X. Wang, R. Ding, R. Raychowdhury, N. Friedman, N. Hacohen, H. Park, A. P. May, and A. Regev, "Single-cell rna-seq reveals dynamic paracrine control of cellular variation," *Nature*, vol. 510, pp. 363 EP –, 06 2014. [Online]. Available: <http://dx.doi.org/10.1038/nature13437>
- [25] R. M. Kumar, P. Cahan, A. K. Shalek, R. Satija, A. Jay DaleyKeyser, H. Li, J. Zhang, K. Pardee, D. Gennert, J. J. Trombetta, T. C. Ferrante, A. Regev, G. Q. Daley, and J. J. Collins, "Deconstructing transcriptional heterogeneity in pluripotent stem cells," *Nature*, vol. 516, pp. 56 EP –, 12 2014. [Online]. Available: <http://dx.doi.org/10.1038/nature13920>
- [26] I. Engel, G. Seumois, L. Chavez, D. Samaniego-Castruita, B. White, A. Chawla, D. Mock, P. Vijayanand, and M. Kronenberg, "Innate-like functions of natural killer t cell subsets result from highly divergent gene programs," *Nature Immunology*, vol. 17, pp. 728 EP –, 04 2016. [Online]. Available: <http://dx.doi.org/10.1038/ni.3437>
- [27] F. Buettner, K. N. Natarajan, F. P. Casale, V. Proserpio, A. Scialdone, F. J. Theis, S. A. Teichmann, J. C. Marioni, and O. Stegle, "Computational analysis of cell-to-cell heterogeneity in single-cell rna-sequencing data reveals hidden subpopulations of cells," *Nature Biotechnology*, vol. 33, pp. 155 EP –, 01 2015. [Online]. Available: <http://dx.doi.org/10.1038/nbt.3102>
- [28] B. Tasic, V. Menon, T. N. Nguyen, T. K. Kim, T. Jarsky, Z. Yao, B. Levi, L. T. Gray, S. A. Sorensen, T. Dolbeare, D. Bertagnolli, J. Goldy, N. Shapovalova, S. Parry, C. Lee, K. Smith, A. Bernard, L. Madisen, S. M. Sunkin, M. Hawrylycz, C. Koch, and H. Zeng, "Adult mouse cortical cell taxonomy revealed by single cell transcriptomics," *Nature Neuroscience*, vol. 19, pp. 335 EP –, 01 2016. [Online]. Available: <http://dx.doi.org/10.1038/nn.4216>
- [29] N. Leng, L.-F. Chu, C. Barry, Y. Li, J. Choi, X. Li, P. Jiang, R. M. Stewart, J. A. Thomson, and C. Kendzierski, "Oscope identifies oscillatory genes in unsynchronized single-cell rna-seq experiments," *Nature Methods*, vol. 12, pp. 947 EP –, 08 2015. [Online]. Available: <http://dx.doi.org/10.1038/nmeth.3549>
- [30] Q. Deng, D. Ramsköld, B. Reinius, and R. Sandberg, "Single-cell rna-seq reveals dynamic, random monoallelic gene expression in mammalian cells," *Science*, vol. 343, no. 6167, pp. 193–196, 2014. [Online]. Available: <http://science.sciencemag.org/content/343/6167/193>
- [31] F. Guo, L. Yan, H. Guo, L. Li, B. Hu, Y. Zhao, J. Yong, Y. Hu, X. Wang, Y. Wei, W. Wang, R. Li, J. Yan, X. Zhi, Y. Zhang, H. Jin, W. Zhang, Y. Hou, P. Zhu, J. Li, L. Zhang, S. Liu, Y. Ren, X. Zhu, L. Wen, Y. Q. Gao, F. Tang, and J. Qiao, "The transcriptome and dna methylome landscapes of human primordial germ cells," *Cell*, vol. 161, no. 6, pp. 1437–1452, 2017/12/05. [Online]. Available: <http://dx.doi.org/10.1016/j.cell.2015.05.015>
- [32] L.-F. Chu, N. Leng, J. Zhang, Z. Hou, D. Mamott, D. T. Vereide, J. Choi, C. Kendzierski, R. Stewart, and J. A. Thomson, "Single-cell rna-seq reveals novel regulators of human embryonic stem cell differentiation to definitive

- endoderm,” *Genome Biology*, vol. 17, no. 1, p. 173, 2016. [Online]. Available: <https://doi.org/10.1186/s13059-016-1033-x>
- [33] S. Darmanis, S. A. Sloan, D. Croote, M. Mignardi, S. Chernikova, P. Samghababi, Y. Zhang, N. Neff, M. Kowarsky, C. Caneda, G. Li, S. D. Chang, I. D. Connolly, Y. Li, B. A. Barres, M. H. Gephart, and S. R. Quake, “Single-cell rna-seq analysis of infiltrating neoplastic cells at the migrating front of human glioblastoma,” *Cell reports*, vol. 21, no. 5, pp. 1399–1410, 10 2017. [Online]. Available: <https://www.ncbi.nlm.nih.gov/pubmed/29091775>
- [34] M. Delmans and M. Hemberg, “Discrete distributional differential expression (d3e) - a tool for gene expression analysis of single-cell rna-seq data,” *BMC Bioinformatics*, vol. 17, no. 1, p. 110, 2016. [Online]. Available: <https://doi.org/10.1186/s12859-016-0944-6>

## APPENDIX A

\*review EBseq model\*

## APPENDIX B

On the Poisson version of modal clust

## APPENDIX C

on randomized clusterings

## APPENDIX D

On the double Dirichlet masses, using notation as in Section 2.3 we have density functions:

$$p_\pi(\phi, \psi) = q_\pi(\Phi_\pi, \Psi_\pi) \prod_{b \in \pi} \left[ p(\tilde{\phi}_b) p(\tilde{\psi}_b) \right]$$

with

$$q_\pi(\Phi_\pi, \Psi_\pi) = \frac{\Gamma(\sum_{b \in \pi} \beta_b)}{\prod_{b \in \pi} \Gamma(\beta_b)} \left[ \prod_{b \in \pi} \Phi_b^{\beta_b - 1} \right] 1[\Phi_\pi = \Psi_\pi]$$

and

$$p(\tilde{\phi}_b) = \frac{\Gamma(\sum_{k \in b} \alpha_k)}{\prod_{k \in b} \Gamma(\alpha_k)} \prod_{k \in b} \tilde{\phi}_k^{\alpha_k - 1}, \quad p(\tilde{\psi}_b) = \frac{\Gamma(\sum_{k \in b} \alpha_k)}{\prod_{k \in b} \Gamma(\alpha_k)} \prod_{k \in b} \tilde{\psi}_k^{\alpha_k - 1}.$$

## APPENDIX E

**Lemma 1.** *If  $\pi_2$  is not refinement of  $\pi_1$  then  $A_{\pi_1} \cap A_{\pi_2}$  is a lower dimensional subset of  $A_{\pi_2}$*

Proof of theorem 2

*Proof.* by lemma 1, it is easy to verify. □

where  $p(t^1, t^2 | \phi, \psi) = p(t^1 | \phi)p(t^1 | \psi)$ ,  $t^1 | \phi \sim \text{multinomial}(n_1, \phi)$ ,  $t^2 | \psi \sim \text{multinomial}(n_2, \psi)$ . Recall the definition of  $A_\pi = \{(\phi, \psi) : \Phi_b = \Psi_b\}$  and  $A_\pi$  is a simplex. Denote the finest partition as  $\pi_F = \{\{1\}, \{2\}, \dots, \{K\}\}$ , associated simplex  $A_{\pi_F} = \{(\phi, \psi) : \phi_i = \psi_i, i = 1, \dots, K\}$  for any two partition  $\pi_1$  and  $\pi_2$ , intersection of their associated simplex must not be empty since  $A_{\pi_F} \subset A_{\pi_1} \cap A_{\pi_2} \neq \emptyset$ . To discuss the issue of overlapping of simplex  $A_\pi$ , we first introduce some notations. The whole space  $\Omega = \{(\phi, \psi), \phi_i, \psi_i > 0 \text{ and } \sum_{i=1}^K \phi_i = \sum_{i=1}^K \psi_i = 1\}$  and we define the refinement and coarseness relationship between partitions, we say a partition  $\tilde{\pi}$  refines another partition  $\pi$  if  $\forall b \in \pi$  there exists  $s \subset \tilde{\pi}$  such that  $\cup_{b' \in s} b' = b$ . When  $\tilde{\pi}$  refines  $\pi$ , we say  $\tilde{\pi}$  is a refinement of (finer than)  $\pi$  or  $\pi$  is a coarseness of (coarser than)  $\tilde{\pi}$ . Observe that if  $\pi'$  refines  $\pi$ , then  $A_\pi \cap A_{\pi'} = A_{\pi'}$ ,  $\int_{A_\pi \cap A_{\pi'}} p(z^1, z^2 | \phi, \psi) p(\phi, \psi | A_{\pi'}) d\phi d\psi = \int_{A_{\pi'}} p(t^1, t^2 | \phi, \psi) p(\phi, \psi | A_{\pi'}) d\phi d\psi$ . When  $\pi'$  is not refinement of  $\pi$ , we need to know the dimension of  $A_\pi \cap A_{\pi'}$ . Consider a map  $f : b \rightarrow v$ , which maps the block  $b$  to a vector  $v \in \{0, 1\}^K$ , the  $i$ th component of  $v$  is  $1_{\{i \in b\}}$ . And denote  $\dim(S)$  be the dimension of space  $S$ .  $A_\pi$  can be equivalently defined as  $A_\pi = \{(\phi, \psi) : M_\pi * (\phi - \psi) = 0\}$ ,  $M_\pi$  is a matrix with rows be  $v_b = f(b), \forall b \in \pi$ , that is to say  $(\phi, \psi)$  are in the null space of linear transformation  $M_\pi$ . We have following lemma

Proof of lemma 1

*Proof.* Let  $V$  denote the orthogonal space of  $\phi - \psi$ , when  $(\phi, \psi) \in A_{\pi_1} \cap A_{\pi_2}$ , and  $\dim(A_{\pi_1} \cap A_{\pi_2}) = \dim(\phi - \psi) + \dim(\psi) = 2K - \dim(V) - 1$ . Also let  $\pi_1 = \{b_1^1, \dots, b_s^1\}$ ,  $\pi_2 = \{b_1^2, \dots, b_t^2\}$ . The corresponding vectors are  $v_1^1, \dots, v_s^1$  and  $v_1^2, \dots, v_t^2$ . We claim there must be a  $b_i^1 \in \pi$  whose corresponding  $v_i^1$  is linear independent with  $v_1^2, \dots, v_t^2$ . If not, for every  $v_i^1$  there exists  $\alpha_1^i, \dots, \alpha_t^i$  such that

$$v_i^1 = \sum_{j=1}^t \alpha_j^i v_j^2 \quad (*)$$

If  $b_j^2 \cap b_i^1 \neq \emptyset$ , then multiply  $v_j^2$  on both sides of (\*), we obtain  $v_i^1 * v_j^2 = \alpha_j^i (v_j^2)^2$ , as  $v_j^2$  are orthogonal vectors, and  $v_i^1 * v_j^2 > 0$  implies  $\alpha_j^i > 0$ . Consider  $x = f(b_j^2 \setminus b_i^1)$ , we have  $x * v_i^1 = 0$  and we multiply  $x$  on both sides of (\*) to obtain  $\alpha_j^i v_j^2 * x = 0$ , thus  $x$  must be zero vector and  $b_j^2 \setminus b_i^1 = \emptyset$ , which implies  $b_j^2 \subset b_i^1$ . That is to say when  $b_j^2 \cap b_i^1 \neq \emptyset$ ,  $b_j^2$  must be subset of  $b_i^1$ . So  $b_i^1$  is union of some blocks in  $\pi_2$ . Which implies  $\pi_2$  is refinement of  $\pi_1$ , contradiction.

Consequently there exists  $b \in \pi_1$  with  $v(b)$  linear independent with  $v(b'), b' \in \pi_2$ .  $\dim(V)$  is at least  $N(\pi_2) + 1$ ,  $\dim(A_{\pi_1} \cap A_{\pi_2}) < \dim(A_{\pi_2})$   $\square$

Proof of theorem 3 and theorem 4

*Proof.* Given the condition that  $\alpha_k = 1, \forall k$  and  $\beta_b = \sum_{k \in b} \alpha_k$ , recall  $p(A_\pi | t^1, t^2) = \sum_{\pi' \in \text{RF}(\pi)} J(t^1, t^2, \pi')$  and  $J(t^1, t^2, \pi) = \frac{1}{c'} \prod_{b \in \pi} \frac{\Gamma(\beta_b + t_b^1 + t_b^2)}{\Gamma(\beta_b + t_b^1) \Gamma(\beta_b + t_b^2)}$

Assuming there are  $K$  subgroups, since  $n_1$  and  $n_2$  goes to infinite at same rate, for simplicity we assume  $n = \sum_{i=1}^K t_i^1 = \sum_{i=1}^K t_i^2$ ,  $t^1 \sim \text{multinomial}(\phi)$ ,  $t^2 \sim \text{multinomial}(\psi)$  and  $t_b^1 = \sum_{i \in b} z_i^1$  and  $t_b^2 = \sum_{i \in b} z_i^2$ , so  $t_b^1 \sim \text{binomial}(n, \Phi_b)$  and  $t_b^2 \sim \text{binomial}(n, \Psi_b)$ , where  $\Phi_b = \sum_{i \in b} \phi_i$  and  $\Psi_b = \sum_{i \in b} \psi_i$ . Let  $f(n, b) = \frac{\Gamma(\beta_b + t_b^1 + t_b^2)}{\Gamma(\beta_b + t_b^1) \Gamma(\beta_b + t_b^2)}$ , then

$$J(z^1, z^2, \pi) \propto \prod_{b \in \pi} f(n, b)$$

$\log f(n, b) = \log(\Gamma(\beta_b + t_b^1 + t_b^2)) - \log(\Gamma(\beta_b + t_b^1)) - \log(\Gamma(\beta_b + t_b^2))$ , notice that  $t_b^1, t_b^2$  and  $\beta_b$  are integers, and when  $x$  is integer,  $\Gamma(x)$  is the factorial of  $(x-1)$ . We have  $\log f(n, b) = \log((\beta_b + t_b^1 + t_b^2 - 1)!) - \log((\beta_b + t_b^1 - 1)!) - \log((\beta_b + t_b^2 - 1)!) = \log((\beta_b + t_b^1 + t_b^2 - 1)!) - \log((\beta_b + t_b^1 - 1)!) - \log((\beta_b + t_b^2 - 1)!) = \log((\beta_b + t_b^1 + t_b^2 - 1)!) - \log((\beta_b + t_b^1 - 1)!) - \log((\beta_b + t_b^2 - 1)!) \approx (\beta_b + t_b^1 + t_b^2 - 1) \log(\beta_b + t_b^1 + t_b^2 - 1) - (\beta_b + t_b^1 - 1) \log(\beta_b + t_b^1 - 1) - (\beta_b + t_b^2 - 1) \log(\beta_b + t_b^2 - 1) + O(\log(n))$ .

Plug into  $f(n, b)$  we have:

$$\log f(n, b) \approx (\beta_b + t_b^1 - 1) \log(1 + \frac{t_b^2}{\beta_b + t_b^1 - 1}) + (\beta_b + t_b^2 - 1) \log(1 + \frac{t_b^1}{\beta_b + t_b^2 - 1}) + O(\log(n))$$

as  $\beta_b \log(\beta_b + t_b^1 + t_b^2 - 1) \sim O(\log(n))$  and by law of large number and slusky's theorem,  $\log(1 + \frac{t_b^2}{\beta_b + t_b^1 - 1}) \rightarrow \log(1 + \frac{\Psi_b}{\Phi_b})$ ,  $\log(1 + \frac{t_b^1}{\beta_b + t_b^2 - 1}) \rightarrow \log(1 + \frac{\Phi_b}{\Psi_b})$  a.s. and  $\frac{\log f(n, b)}{n} \rightarrow \Phi_b \log(1 + \frac{\Psi_b}{\Phi_b}) + \Psi_b \log(1 + \frac{\Phi_b}{\Psi_b})$  a.s. We have:

$$\frac{\log(\prod_{b \in \pi} f(n, b))}{n} \rightarrow \sum_b [\Phi_b \log(1 + \frac{\Psi_b}{\Phi_b}) + \Psi_b \log(1 + \frac{\Phi_b}{\Psi_b})] \quad a.s.$$

To find the maxima  $(\Phi, \Psi)$ , we fix  $\Psi$  and let  $C = \frac{\log(\prod_{b \in \pi} f(n, b))}{n} + \lambda(\sum_{b \in \pi} \Phi_b - 1)$ , we have

$\frac{\partial C}{\partial \Phi_b} = \log(1 + \frac{\Psi_b}{\Phi_b}) + \lambda$ , stationary point is  $\Phi_b = \Psi_b, \forall b$ . and for the hessian matrix  $\frac{\partial^2 C}{\partial \Phi_b^2} = -\frac{\Psi_b}{\Phi_b^2 + \Phi_b \Psi_b} < 0$  and  $\frac{\partial^2 C}{\partial \Phi_b \partial \Phi_{b'}} = 0$ , if  $b \neq b'$ , that is to say the hessian matrix is a diagonal matrix with every diagonal elements to be negative, so it is negative definite, and our objective function is concave. The maxima is the stationary point  $\Phi = \Psi$ . And when  $\Phi = \Psi$ ,  $\frac{\log(\prod_{b \in \pi} f(n, b))}{n} = 2 \ln(2)$  a constant not dependent on partition  $\pi$  and  $\Phi$ . That is to say if  $(\phi, \psi) \in A_{\pi_1} \cap A_{\pi_2}$  and  $(\phi, \psi) \notin A_{\pi_3}$ . Then we would have  $\lim_{n \rightarrow \infty} \frac{\log(\prod_{b \in \pi_1} f(n, b))}{n} = \lim_{n \rightarrow \infty} \frac{\log(\prod_{b \in \pi_2} f(n, b))}{n}$  and  $\lim_{n \rightarrow \infty} [\frac{\log(\prod_{b \in \pi_1} f(n, b))}{n} - \frac{\log(\prod_{b \in \pi_3} f(n, b))}{n}] = c > 0$ , which implies:

$$(A) \quad \frac{J(t^1, t^2, \pi_3)}{J(t^1, t^2, \pi_1)} \rightarrow 0 \quad a.s.$$

To investigate the limit of  $\frac{J(t^1, t^2, \pi_1)}{J(t^1, t^2, \pi_2)}$ , We use inequalities that  $\sqrt{2\pi} n^{n+\frac{1}{2}} e^{-n} \leq n! \leq e n^{n+\frac{1}{2}} e^{-n}$  holds for all nonnegative integers  $n$ . Plug in  $f(n, b)$ , we have:

$$(1) \quad \beta_b + \log\sqrt{2\pi} - 3 + g(n, b) \leq f(n, b) \leq \beta_b - 2\log\sqrt{2\pi} + g(n, b)$$

$$g(n, b) = (\beta_b + t_b^1 - \frac{1}{2})\log(1 + \frac{t_b^2}{\beta_b + t_b^1 - 1}) + (\beta_b + t_b^2 - \frac{1}{2})\log(1 + \frac{t_b^1}{\beta_b + t_b^2 - 1}) - (\beta_b - \frac{1}{2})\log(\beta_b + t_b^1 + t_b^2 - 1)$$

Based on inequalities (1),  $\sum_{b \in \pi} f(n, b)$  only differ with  $\sum_{b \in \pi} g(n, b)$  by a constant. By Taylor's expansion  $\log(1 + x) = \log 2 + \frac{1}{2}(x - 1) + O((x - 1)^2)$ , we have  $\log(1 + \frac{t_b^2}{\beta_b + t_b^1 - 1}) = \log 2 + \frac{1}{2}(\frac{t_b^1 - t_b^2 + 1 - \beta_b}{\beta_b + t_b^1 - 1}) + O_p((\frac{t_b^1 - t_b^2 + 1 - \beta_b}{\beta_b + t_b^1 - 1})^2)$  and under condition  $\Phi_b = \Psi_b, \frac{(t_b^1 - t_b^2 + 1 - \beta_b)^2}{\beta_b + t_b^1 - 1}$  is  $O_p(1)$ . Plug in  $g(n, b)$

$$g(n, b) = \log 2 * t_b^1 + \log 2 * t_b^2 - (\beta_b - \frac{1}{2})\log(\beta_b + t_b^1 + t_b^2 - 1) + O_p(1)$$

and sum up

$$(2) \quad \sum_{b \in \pi} g(n, b) = 2n\log 2 - \sum_{b \in \pi} (\beta_b - \frac{1}{2})\log(\beta_b + t_b^1 + t_b^2 - 1) + O_p(1)$$

Notice that when two partition  $\pi_1, \pi_2$  have same number of blocks  $b$  and  $\Phi_b = \Psi_b, \forall b \in \pi_1 \cup \pi_2$ ,

$$\begin{aligned} \sum_{b \in \pi_1} g(n, b) - \sum_{b' \in \pi_2} g(n, b') &= \sum_{b' \in \pi_2} (\beta'_b - \frac{1}{2})\log(\beta'_b + t_{b'}^1 + t_{b'}^2 - 1) - \sum_{b \in \pi_1} (\beta_b - \frac{1}{2})\log(\beta_b + t_b^1 + t_b^2 - 1) + O_p(1) \\ &= \sum_{b' \in \pi_2} (\beta_{b'} - \frac{1}{2})\log(\frac{\beta'_b + t_{b'}^1 + t_{b'}^2 - 1}{n}) - \sum_{b \in \pi_1} (\beta_b - \frac{1}{2})\log(\frac{\beta_b + t_b^1 + t_b^2 - 1}{n}) \\ &\quad + \sum_{b' \in \pi_2 - \frac{1}{2}} (\beta_{b'} - \frac{1}{2})\log(n) - \sum_{b \in \pi_1 - \frac{1}{2}} (\beta_b - \frac{1}{2})\log(n) + O_p(1) \\ &= O_p(1) + \sum_{b \in \pi_1} \frac{1}{2}\log(n) - \sum_{b' \in \pi_2} \frac{1}{2}\log(n) \\ &= O_p(1) \end{aligned}$$

When  $\pi_1$  and  $\pi_2$  have same number of blocks,

$$(B) \quad \frac{J(t^1, t^2, \pi_1)}{J(t^1, t^2, \pi_2)} \rightarrow O_p(1) \quad a.s.$$

When  $\pi_1$  have less blocks than  $\pi_2$ ,  $\sum_{b' \in \pi_2} g(n, b') - \sum_{b \in \pi_1} g(n, b) = O_p(\log(n))$

$$(C) \quad \frac{J(t^1, t^2, \pi_1)}{J(t^1, t^2, \pi_2)} \rightarrow 0 \quad a.s.$$

□

*Email address:* `newton@biostat.wisc.edu`